ELSEVIER

Journal of Organometallic Chemistry 522 (1996) 33–38

Journal of Organometallic Chemistry

Synthesis, ^{31}P NMR data and X-ray analysis of a ruthenium(II) dimethylphenylphosphine complex with dimerized phenylacetylene: the structure of $[(PhMe_2P)_4Ru(\eta^3\text{-}PhC_3CHPh)](PF_6)$

David C. Liles [a], Paul F.M. Verhoeven [b,*]

[a] *Materials Science and Technology, CSIR, PO Box 395, Pretoria 0001, South Africa*
[b] *Department of Chemistry, University of Stellenbosch, Stellenbosch 7600, South Africa*

Received 11 September 1995

Abstract

Treatment of $[RuHL_5]^+$ (L = PMe_2Ph) with phenylacetylene in ethanol yielded the dimerization of HC≡CPh to (*Z*)-1,4-diphenylbut-3-en-1-yne. The molecular structure of $[Ru(\eta^3\text{-}PhC_3CHPh)L_4](PF_6)$ (L = PMe_2Ph) (**2**) shows a seven-coordinate environment at ruthenium; the η^3-butenynyl moiety is both σ- and π-coordinated to the metal centre. Low-temperature ^{31}P NMR data for some $[Ru(C{\equiv}CR)L_3](PF_6)$ complexes with R = Ph, CO_2Et, $SiMe_3$, ^{t}Bu and L = PMe_2Ph are discussed.

Keywords: Ruthenium; ^{31}P NMR; X-ray diffraction; Crystal structure; Alkyne dimerization

1. Introduction

Cationic five-coordinated ruthenium systems of general formula $[RuX_nL_{5-n}]^+$ (n = 1 or 2) where X stands for hydride and/or unsaturated hydrocarbons and L mono or chelating multidentate phosphine ligands, are important intermediates in the selective homogeneous hydrogenation and polymerization of olefins and acetylenes [1]. The catalytic properties of such ruthenium complexes depend on the facile removal of the alkenyl/alkynyl functionality which is an essential requisite for the occurrence of any catalytic cycle as this provides a free coordination site for the incoming hydrocarbon molecule. Ruthenium hydrido–diene phosphine complexes are reactive towards a series of neutral donor ligands of Groups IV(14) and V(15), as has been investigated by Singleton and coworkers [2]. Reactivity and fluxional behaviour of these complexes is understood in terms of (1) the coordinatively unsaturated metal centre, (2) the lability of intermediate complexes and (3) steric effects of the phosphine ligands.

In the quest for the design of highly functional materials, the polymerization of acetylene derivatives has received renewed attention in polymer science [3]. Polyacetylenes are of interest because of their unique properties such as optical and magnetic susceptibility. Although Group VII(9) metal complexes are known to initiate stereospecific polymerization of alkylated acetylenes in almost quantitative yields, efficient methods of polymerization remain open to further investigation. Recently, Japanese researchers have accomplished the first living polymerization of phenylacetylene using a rhodium–olefin complex [4]. To understand the mechanism and factors that govern stereoselectivity at the coordination sphere of transition metal centres, detailed mechanistic studies on the interaction between the metal and the alkyne as well as on the 1-alkyne dimerization processes have been undertaken and are widely documented in recent organometallic literature. Bianchini and coworkers have reported on the regio- and stereoselective dimerization of HC≡CR (R = Ph, $SiMe_3$) to (*Z*)-1,4-disubstituted-but-3-en-1-ynes mediated by Ru(II) [5a,5c] and Os(II) [5b] precursors. Wakatsuki et al. [6] performed molecular orbital studies on the selective coupling of terminal alkynes, establishing the mechanism. The catalytic dimerization reactions proceed first via isomerization of the 1-alkyne into the vinylidene form (reported by Werner and coworkers [7] for other platinum group metal complexes) followed by the C–C coupling of the α-carbons of *cis*-vinylidene and alkynyl ligands.

* Corresponding author.

Elsevier Science S.A.
PII S0022-328X(96)06189-X

Unusual structures, all derived directly or indirectly from the interaction of phenylacetylene with various ruthenium complexes, have been reported by Singleton and coworkers [8]. The present study was carried out in order to (1) characterize the product when $[Ru(C{\equiv}CPh)(PMe_2Ph)_4]^+$ reacts with non-activated phenylacetylene, (2) to ascertain the geometry around the steric crowded ruthenium centre (in solution as well as in the solid phase) and (3) to compare ^{31}P NMR data with in situ prepared monosubstituted akynyl complexes of the type $[Ru(C{\equiv}CR)(PMe_2Ph)_4]^+$ where R = CO_2Et, $SiMe_3$, ^tBu and Ph. Herein we report the molecular structure of $[Ru\{\eta^3\text{-}PhCCCC(H)Ph\}(PMe_2Ph)_4](PF_6)$ [9].

2. Results and discussion

The role of five-coordinated σ-alkynyl and π-alkenyl Ru(II) compounds in the dimerization reactions of terminal alkynes is important to rationalize the catalysis cycle. In recent literature acetylide and vinyl metal complexes are considered key intermediates for the synthesis of butenynyl derivatives [10]. Bianchini et al. [5c] demonstrated that $[Ru(HC{\equiv}CPh)(PP_3)]$ with PP_3 the tripodal tetradentate ligand $P(CH_2CH_2PPh_2)_3$ is the most likely π-alkyne intermediate for the formation of air-stable bis(alkynyl) catalyst precursor $[(PP_3)Ru(C{\equiv}CPh)_2]$.

The fluxional behaviour exhibited by coordinatively unsaturated Group VIII complexes with bulky phosphines in solution was the subject of several experimental [11] and theoretical studies which set out to establish their stereochemistry. The calculated energy difference between a square-pyramidal and trigonal-bipyramidal structure for five-coordinated d^6 metal complexes is small but nevertheless favours the former as the more stable geometry [12]. Ashworth et al. [13] provided the first direct experimental evidence for the square-pyramidal geometry based on 32 MHz ^{31}P NMR studies of $[RuXL_4]^+$ and $[RuX(L_2)_2]^+$ (X = H, C_2Ph; L = PMe_2Ph; L_2 = $(Ph_2PCH_2)_2CH_2$).

2.1. ^{31}P NMR data

The solution dynamics of $[Ru(C{\equiv}CR)L_4]^+$ complexes were investigated by variable temperature $^{31}P\{^1H\}$ NMR spectroscopy. The salts $[Ru(C{\equiv}CR)L_4](PF_6)$ (L = PMe_2Ph; R = CO_2Et, $SiMe_3$, ^tBu, Ph), prepared in situ by reacting $[RuHL_5](PF_6)$ with the appropriate acetylene, are listed in Table 1. The ^{31}P NMR results were interpreted as first-order systems. The room temperature $^{31}P\{^1H\}$ NMR spectrum of $[Ru(C{\equiv}CCO_2Et)(PMe_2Ph)_4]^+$ (**3**) exhibits three signals of relative intensity 1:2:1 at δ 21.9 (dt), 0.7 (dd) and −11.3 (dt) ppm. The data are interpreted by assuming an AM_2Q splitting pattern, attributed to the P nuclei of two magnetically equivalent and two non-equivalent phosphine groups. It is reasonable to propose a pseudo-octahedral geometry for compound **3** in which the ruthenium is six-coordinate with two *trans* dimethylphenylphosphine ligands, the third phosphine *trans* to a π-coordinated acetylene functionality and the fourth phosphine *trans* to the carboxyl group of the carbethoxy substituent. Structures in which the carbonyl oxygen of ester groups coordinates to the ruthenium have been reported [10].

The cation $[Ru(C{\equiv}CSiMe_3)(PMe_2Ph)_4]^+$ (**4**) shows a single ^{31}P resonance (δ 10 ppm) at room temperature in acetone which separates at lower temperature into three signals of intensity 1:2:1 and at −60°C it is resolved into three multiplets characterized by the parameters in Table 1. The band-line widths are still too large to distinguish between the values of J_{MQ} and J_{AQ}. Similarly the cations $[Ru(C{\equiv}C^tBu)(PMe_2Ph)_4]^+$ (**5**) and $[Ru(C{\equiv}CPh)(PMe_2Ph)_4]^+$ (**1**) exhibit fast-exchange spectra at ambient temperature. Upon a decrease in temperature, the fluxional behaviour slows down and an AM_2Q type pattern starts to appear.

The ^{31}P NMR spectrum of **2** taken in acetone (85% H_3PO_4 as the external standard) at room temperature shows a major broad singlet at δ −1.6 ppm, which separates at −20°C into well-resolved signals of intensity 1:2:1. The spectra shown in Fig. 1 have been simulated using an AM_2Q spin system and the following coupling constants: J_{AM} = 32.8, J_{MQ} = 26.2 and J_{AQ} = 17.4 Hz. The NMR results indicate that **2** has two

Table 1
^{31}P NMR data for $[RuX(PMe_2Ph)_4](PF_6)$ complexes

	X	CN [a]	T [b]	δ_X [c]	δ_M	δ_Q	J_{AM} [d]	J_{MQ}	J_{AQ}
3	$C{\equiv}CCO_2Et$	6	303	21.9(dt)	0.7(dd)	−11.3(dt)	33.9	25.3	18.7
4	$C{\equiv}CSiMe_3$	5	213	28.8(m)	−0.2(m)	−7.4(m)	34	26	26
5	$C{\equiv}C^tBu$	5	200	30.1(q)	0.9(t)	−5.8(q)	31	26	26
1	$C{\equiv}CPh$	5	225	26.4(m)	0.6(m)	−6.9(m)	33	26	26
2	PhC_3CHPh	6	253	10.4(dt)	−4.3(dd)	−10.1(dt)	33	26	17

[a] Coordination number around Ru^{II}. [b] Temperature in kelvin. [c] Chemical shifts relative to external H_3PO_4.
[d] Coupling constants in Hertz.

magnetically equivalent P nuclei (labelled M) and two non-equivalent P nuclei (labelled A and Q). The IR spectrum of **2** shows diagnostic bands at 2058 cm^{-1} assigned to $\nu(C{\equiv}C)$ and at 1590 cm^{-1} to $\nu(C{=}C)$ vibration. On the basis of these data alone, we cannot propose a definitive structure of **2**, and a single-crystal X-ray diffraction study was therefore undertaken.

2.2. *The crystal structure fo [Ru(PMe$_2$Ph)$_4$(η^3-PhC$_3$CHPh)] (PF$_6$) (2)*

The molecular structure of the complex cation of **2** is illustrated in Fig. 2. The ruthenium (II) atom is in effect seven-coordinate, bonded to four phosphorus atoms of the PMe_3Ph ligands and three carbon atoms of the trihapto bonded 1,4-diphenylbut-3-en-1-ynyl ligand. As with similar structurally characterized Ru complexes [5a,14], the coordination geometry of the cation is a distorted octahedron with one pair of *trans*-phosphines [P(1)–Ru–P(2)], one unique phosphine [P(4)] which is *trans* to the π-bonded [C(51)–C(52)] moiety of the butenynyl group. The other phosphine [P(3)] could be regarded as *trans* to the σ-bonded C(53) atom.

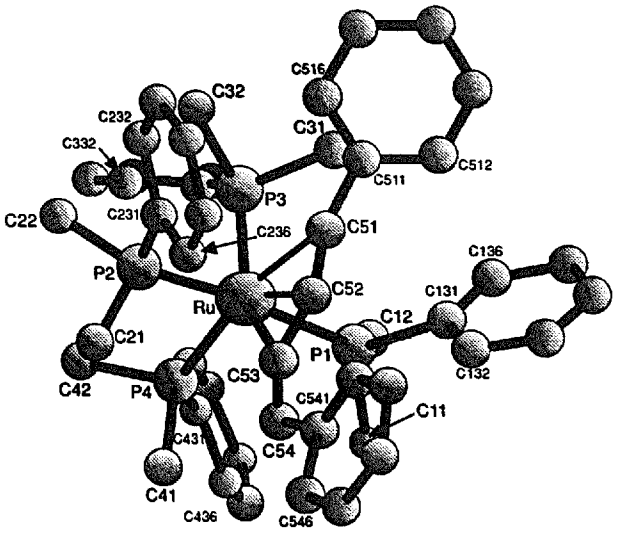

Fig. 2. A perspective drawing of **2** showing the atomic numbering scheme. Hydrogen atoms are omitted for clarity.

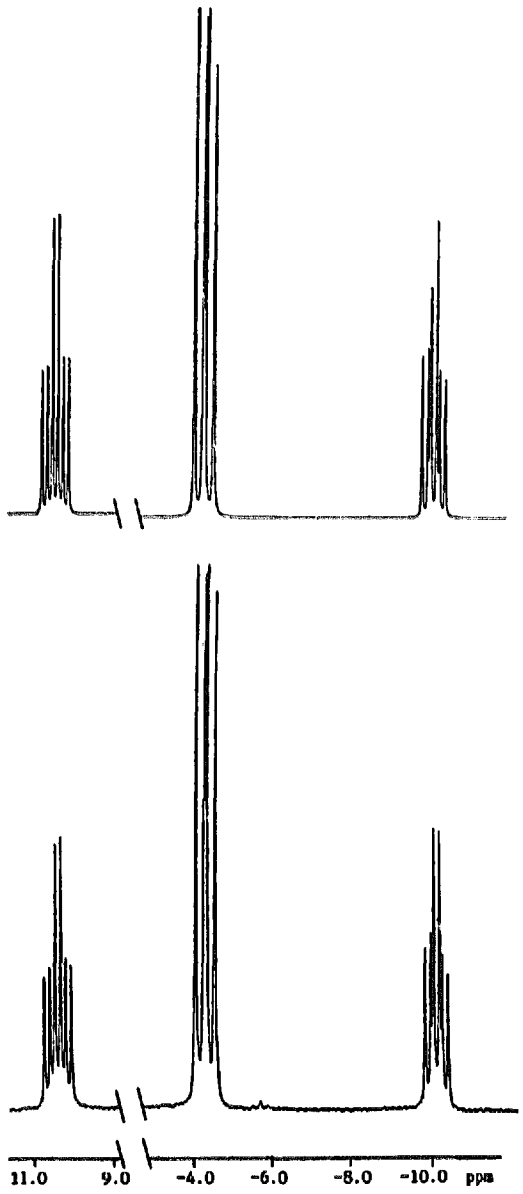

Fig. 1. Observed (bottom) and calculated (top) $^{31}P\{^1H\}$ NMR spectra of [Ru(PMe$_2$Ph)$_4$(η^3-PhC$_3$CHPh)](PF$_6$) (**2**).

Final atomic coordinates with equivalent isotropic displacement parameters are listed in Table 2. Selected bond distances and angles are given in Table 3. The Ru–C(51), Ru–C(52) and Ru–C(53) bond lengths of 2.51, 2.23 and 2.12 Å respectively agree well with the values of 2.49, 2.23 and 2.14 Å reported for the strained cation $[Ru(PP_3)(\eta^3\text{-}Si(Me)_3C_3CHSi(Me)_3)]^+$ with PP_3 = $P(CH_2CH_2PPh_2)_3$ [5a]. The closest interaction with the metal centre is through the C(53) atom, the bond distance of 2.119(4) Å is within the range 2.02–2.20 Å typical for Ru–C single bonds but is significantly longer than those of a majority of ruthenium σ-vinyl complexes [2.034(5)–2.082(6) Å] [15]. The weakest interaction is at the Ru–C(51) bond [2.510(4) Å]. This originates from non-bonded repulsions between the phenyl group bonded to C(51) and groups on the neighbouring phosphine ligands. The existence of steric effects in coordination complexes with PMe_2Ph ligands, caused by large repulsions between the methyl and phenyl groups on different phosphine ligands, has been demonstrated by Singleton and coworkers [16].

The mean Ru–P [2.39 Å] bond length in **2** is longer than the 2.31 Å for a single bond estimated from Pauling's covalent radii reflecting that metal-to-phosphorus bond lengths increase with the build-up of steric demands of tertiary phosphine ligands. This compares well with the two *trans* Ru–P bond distances [2.374(6)

Table 2
Atomic fractional coordinates ($\times 10^4$) and equivalent isotropic displacement parameters ($Å^2 \times 10^3$) for [Ru(PMe_2Ph)$_4$(η^3-PhC_3CHPh)](PF_6)

Atom	x	y	z	U_{eq} [a]
Ru [b]	2278(3)	17772(2)	24260(2)	241(1)
P(1) [b]	9696(8)	23431(7)	36327(6)	284(2)
C(11)	1241(4)	1418(4)	4643(3)	41(1)
C(12)	928(4)	3626(4)	3896(3)	42(1)
C(131)	−611(3)	2390(3)	3715(2)	30(1)
C(132)	−975(3)	1423(3)	3948(2)	37(1)
C(133)	−2167(4)	1432(3)	4085(3)	44(1)
C(134)	−3009(4)	2393(4)	4003(3)	48(1)
C(135)	−2661(4)	3363(4)	3754(3)	46(1)
C(136)	−1467(3)	3356(3)	3611(3)	40(1)
P(2) [b]	35965(9)	8635(8)	13537(6)	334(2)
C(21)	4575(4)	−423(4)	1777(3)	48(1)
C(22)	4664(4)	1501(4)	556(3)	46(1)
C(231)	2867(3)	378(3)	692(2)	36(1)
C(232)	2749(4)	886(3)	−144(3)	40(1)
C(233)	2202(4)	486(4)	−631(3)	53(1)
C(234)	1782(5)	−423(4)	−291(4)	74(2)
C(235)	1899(5)	−938(4)	542(3)	77(2)
C(236)	2433(4)	−548(4)	1023(3)	56(1)
P(3) [b]	20053(8)	35759(7)	15467(6)	299(2)
C(31)	475(4)	4351(3)	1668(3)	41(1)
C(32)	2227(4)	3657(4)	399(3)	46(1)
C(331)	2812(3)	4579(3)	1572(2)	31(1)
C(332)	3981(4)	4494(3)	1173(3)	40(1)
C(333)	4605(4)	5232(4)	1199(3)	53(1)
C(334)	4077(4)	6080(4)	1603(3)	56(1)
C(335)	2919(5)	6183(3)	1992(3)	50(1)
C(336)	2292(4)	5445(3)	1976(2)	40(1)
P(4) [b]	38854(8)	16200(8)	30941(6)	331(2)
C(41)	4356(4)	278(4)	3770(3)	48(1)
C(42)	5300(4)	1758(4)	2447(3)	46(1)
C(431)	3859(3)	2504(3)	3812(2)	35(1)
C(432)	3955(4)	3575(4)	3473(3)	43(1)
C(433)	3978(4)	4260(4)	3983(3)	57(1)
C(434)	3875(5)	3898(5)	4853(3)	67(2)
C(435)	3788(4)	2856(5)	5200(3)	62(1)
C(436)	3789(4)	2160(4)	4693(3)	44(1)
C(51)	551(3)	1561(3)	1874(2)	36(1)
C(52)	1030(3)	798(3)	2395(2)	30(1)
C(53)	1870(3)	248(3)	2942(2)	30(1)
C(54)	2062(3)	−760(3)	3419(2)	34(1)
C(511)	−345(3)	2158(3)	1341(2)	32(1)
C(512)	−1496(4)	2534(3)	1719(3)	44(1)
C(513)	−2359(4)	3121(4)	1217(3)	52(1)
C(514)	−2092(4)	3335(4)	345(3)	52(1)
C(515)	−959(4)	2965(3)	−30(3)	46(1)
C(516)	−87(4)	2380(3)	459(3)	39(1)
C(541)	1412(3)	−1587(3)	3488(2)	36(1)
C(542)	1771(4)	−2608(3)	4005(3)	44(1)
C(543)	1182(5)	−3411(3)	4079(3)	56(1)
C(544)	243(5)	−3240(4)	3661(3)	59(1)
C(545)	−121(4)	−2242(4)	3151(3)	62(1)
C(546)	455(4)	−1421(3)	3066(3)	50(1)
P(5) [b]	27693(12)	34408(9)	77284(8)	557(3)
F(1)	2998(3)	2299(2)	7474(2)	86(1)
F(2)	3611(2)	2897(2)	8442(2)	75(1)
F(3)	2519(3)	4569(2)	7985(2)	98(1)
F(4)	1938(3)	3968(2)	7017(2)	108(1)
F(5)	3862(3)	3703(3)	7069(2)	104(1)
F(6)	1680(2)	3159(2)	8396(2)	95(1)

[a] U_{eq} is defined as one third of the trace of the orthogonalized U_{ij} tensor. [b] Atomic coordinates $\times 10^5$, displacement parameters $\times 10^4$.

and 2.412(6) Å] [17] of the five-coordinate complex [$RuCl_2(PPh_3)_3$]. The Ru–P bond lengths decrease as the steric requirements of the phosphine ligands lessen; as observed in related ruthenium(II) complexes with primary and secondary phosphines. For example, the structure of *trans*-[$RuCl_2(PPhH_2)_4$] shows precisely coplanar equatorial $PPhH_2$ ligands with the ruthenium atom on a crystallographic inversion centre, Ru–P bond lengths of 2.319(3) and 2.318(3) Å and no significant bond angle distortions around Ru^{II} [18].

The C–C bond distances within the η^3-butenynyl ligand are suggestive of some degree of electronic delocalization. The bond distance between C(51) and C(52) [1.229(5) Å] is at the lower end of carbon–carbon triple-bond lengths for π-acetylene complexes, generally observed to range from 1.22 to 1.32 Å [19], and compares extremely well with the value of 1.23(2) Å reported for [Ru{η^3-(*p*-tolyl)C_3CH(*p*-tolyl)}(PhP-$(OEt)_2\}_4$]BPh_4 [10]. The bond lengths of C(52)–C(53) [1.401(5) Å] and C(53)–C(54) [1.341(5) Å] are similar to the C–C distances of 1.379(5), 1.339(5) Å and 1.39(2), 1.33(2) Å respectively reported for Ru(C≡CPh)(η^3-PhC_3CHPh)(Cyttp) with Cyttp = $PhP\{CH_2CH_2CH_2P(c\text{-}C_6H_{11})_2\}_2$ [14] and [Ru{η^3-(*p*-tolyl)C_3CH(*p*-tolyl)}$\{PhP(OEt)_2\}_4$ | BPh_4 [10]. The C(53)–C(54) bond distance of 1.341(5) Å is typical of C=C bonds and compares well with the value of 1.349(8) Å reported for the vinyl hydride complex (PP_3)RuH{η^1-$C(CO_2Me)$=$CH(CO_2Me)$} [5c].

In comparison with other ruthenium complexes, the acetylenic group of the PhC_3CHPh fragment is weakly bound to the metal atom as indicated by the long Ru–C(51) and Ru–C(52) bonds and short C(51)≡C(52) bond distances. An indication of the bonding interaction between Ru and the acetylenic group is given by the bent-back angle C(511)–C(51)–C(52) of 155.8(4)°. Bent-back angles have been reported to range from 168° to 134° for the π-bonded acetylenes in several complexes [19]. The bent-back angle for C(511)–C(51)–C(52) is in good agreement with that reported [156.7(3)°] for *syn-mer*-RuCl(η^3-PhC_3CHPh)(Cyttp) [14].

3. Experimental details

3.1. General and starting materials

Details of the preparation of the starting material [$RuH(PMe_2Ph)_5$](PF_6) have been reported elsewhere [16]. The IR spectrum of the precursor exhibits a band at 1905 cm^{-1} characteristic of the ν(Ru–H). All synthetic work was carried out under an inert atmosphere using standard Schlenk techniques. Solvents used were dried over appropriate drying agents and degassed on a vacuum line. Phenylacetylene was obtained commercially and not purified before use. $^{31}P\{^1H\}$ NMR spectra

were recorded on a Bruker AM300 spectrometer operating at 121.50 MHz. Chemical shifts are relative to external 85% H_3PO_4 with downfield values reported as positive.

3.2. Reaction of $[RuH(PMe_2Ph)_5](PF_6)$ with 1-alkynes for NMR experiments

Solid $[RuH(PMe_2Ph)_5](PF_6)$ (1 g, 1.1 mmol) was dissolved in 10 ml CD_2Cl_2, degassed under argon and kept as a stock solution under refrigeration. Aliquot amounts (0.5 ml) from the stock solution were transferred into 5 mm NMR tubes. One equivalent of the appropriate substituted acetylene (0.055 mmol) was added via syringe to each tube, which was then introduced into the spectrometer. The $^{31}P\{^1H\}$ NMR spectra showed quantitative conversion of $[RuHL_5]^+$ to the alkynyl complexes $[Ru(C{\equiv}CR)L_4]^+$. No attempt was made to characterise minor by-products as we were essentially interested in the interaction of a sterically strained ruthenium hydride phosphine species with added 1-alkyne.

3.3. Synthesis of $[Ru(PMe_2Ph)_4\{\eta^3\text{-}PhCCCC(H)Ph\}](PF_6)$ (2)

3.3.1. Method A

An excess of neat phenylacetylene (0.5 ml, 4.5 mmol) was added to an ethanolic solution (30 ml) of $[RuH(PMe_2Ph)_5](PF_6)$ (1 g, 1.1 mmol). The solution was gently heated to reflux temperature and left stirring for 2 h. A yellow suspension was obtained. The yellow solid was filtered from the cooled solution in almost quantitative yield (recovery 90%). The crude product was recrystallized from dichloromethane/methanol, from which suitable crystals for X-ray analysis were separated.

3.3.2. Method B

Alternatively, **2** could also be prepared by reaction of $[Ru(C{\equiv}CPh)(PMe_2Ph)_4](PF_6)$ (**1**) (0.45 g, 0.5 mmol) with a slight excess of HC≡CPh (66 μl, 0.6 mmol) at room temperature in dichloromethane (20 ml). After 60 min of stirring, the addition of ethanol (20 ml) followed by slow concentration caused a precipitation of a yellow solid in almost quantitative yield (at least 90%).

3.4. Single-crystal structure determination

The intensity data were collected on an Enraf-Nonius CAD-4F diffractometer at 275 K, using graphite monochromated Mo Kα radiation ($\lambda = 0.71069$ Å). The data were corrected for absorption by the semi-empirical method of North et al. [20]. Crystal data, data collection parameters and results of the analysis are given in Table 4. The structure was solved by a combination of Patterson and difference Fourier methods. The final R value was 0.0404, $R_w = 0.029$ using 6457 reflections with $F_o \geq 4\sigma(F_o)$ and anisotropic thermal parameters for all the non-hydrogen atoms. The hydrogen atoms were all located in their idealized positions (C–H bond value of 0.96 Å) and included in structure factor calculations as well as in refinement. Refinement was by blocked-matrix weighted least-squares. The SHELX-76 program was used for all the calculations [21]. Lists of anisotropic temperature factors for non-hydro-

Table 3
Selected bond lengths (Å) and angles (°) for $[Ru(PMe_2Ph)_4(\eta^3\text{-}PhC_4CHPh)](PF_6)$

Ru–P(1)	2.395(1)	C(51)–C(52)	1.229(5)		
Ru–P(2)	2.425(1)	C(51)–C(511)	1.445(5)		
Ru–P(3)	2.411(1)	C(52)–C(53)	1.401(5)		
Ru–P(4)	2.324(1)	C(53)–C(54)	1.341(5)		
Ru–C(51)	2.510(4)	C(54)–C(541)	1.464(6)		
Ru–C(52)	2.226(4)				
Ru–C(53)	2.119(4)				
P(1)–Ru–P(2)	169.3(1)	P(2)–Ru–P(3)	96.0(1)	P(3)–Ru–P(4)	103.0(1)
P(1)–Ru–P(3)	94.5(1)	P(2)–Ru–P(4)	89.8(1)	P(3)–Ru–C(51)	87.9(1)
P(1)–Ru–P(4)	89.5(1)	P(2)–Ru–C(51)	89.0(1)	P(3)–Ru–C(52)	117.2(1)
P(1)–Ru–C(51)	89.5(1)	P(2)–Ru–C(52)	86.5(1)	P(3)–Ru–C(53)	154.7(1)
P(1)–Ru–C(52)	87.0(1)	P(2)–Ru–C(53)	84.3(1)	P(4)–Ru–C(51)	168.3(1)
P(1)–Ru–C(53)	85.4(1)			P(4)–Ru–C(52)	139.0(1)
				P(4)–Ru–C(53)	101.5(1)
C(51)–Ru–C(52)	29.3(1)	C(51)–Ru–C(53)	66.8(1)	C(52)–Ru–C(53)	37.5(1)
Ru–C(51)–C(52)	62.4(3)	Ru–C(51)–C(511)	141.4(3)	Ru–C(52)–C(53)	67.1(2)
Ru–C(52)–C(51)	88.3(3)	Ru–C(53)–C(54)	153.4(3)	Ru–C(53)–C(52)	75.4(2)
C(511)–C(51)–C(52)	155.8(4)	C(51)–C(52)–C(53)	155.3(4)	C(52)–C(53)–C(54)	131.1(4)

Table 4
Crystallographic and collection data for $[(PhMe_2P)_4Ru(\eta^3\text{-}PHC_3CHPh)](PF_6)$

Molecular formula	$C_{48}H_{55}F_6P_5Ru$
Formula weight	1001.90
Crystal system	Triclinic
Space group	$P\bar{1}$ (No. 2)
Unit cell parameters	$a = 11.873(3)$ Å $\alpha = 75.59(2)°$
	$b = 13.099(3)$ Å $\beta = 78.36(2)°$
	$c = 16.396(3)$ Å $\gamma = 74.05(2)°$
	$V = 2350.03$ Å^3 $Z = 2$
Density (calc.)	1.416 Mg m^{-3}
Crystal dimensions	$0.27 \times 0.13 \times 0.14$ mm^3
Data collection	Temperature: 275 ± 1 K, 8230 reflections measured
Collection range	$3 \le \theta \le 25°$, h 0 → 14, k −15 → 15, l −19 → 19
Scan type and angle	ω–2θ; $(0.56 + 0.35 \tan \theta)$
Scan speed	Variable, max. 0.0915° s^{-1}, max. time 50 s/reflection
Detector aperture	$(1.25 + 0.50 \tan \theta)$ mm (horiz.) × 4.0 mm (vert.)
Intensity controls	3, (016), (036) and (253) measured every 60 min
X-ray exposure time	49 h, average total change in intensity −1.7%
Structure solution and refinement	
Refinement	Blocked-matrix weighted least-squares (four blocks) $\Sigma w(\Delta F)^2$ minimized, $w = \sigma^{-2}(F)$
No. of parameters refined	711
Final R indices	$R = 4.04\%$, $R_w = 2.9\%$
Residual electron density	Max. 0.376, min. −0.326 e Å^{-3}

gen atoms and atom coordinates and isotropic thermal parameters for hydrogen atoms have been deposited at the Cambridge Crystallographic Data Centre.

4. Summary

The reaction of $[RuH(PMe_2Ph)_5]^+$ with phenylacetylene under mild conditions gives the unique compound $[Ru(\eta^3\text{-}PhCCCC(H)Ph)(PMe_2Ph)_4](PF_6)$ which contains the metal-bound η^3-PhCCCC(H)Ph carbon–carbon coupling product of phenylacetylene. $^{31}\{^1H\}$ NMR data in solution are consistent with the results of an X-ray single-crystal structure determination.

Acknowledgements

PFMV is grateful to the CSIR for providing him with the opportunity to publish this work. This paper is dedicated to Drs. T.V. Ashworth and E. Singleton of the former National Chemical Research Laboratory at the CSIR, South Africa for their outstanding contributions made in the field of ruthenium organometallic chemistry. The authors wish to thank the referees and Professor J.R. Moss for valuable comments.

References

[1] F.A. Cotton, G. Wilkinson and P.L. Gaus, *Basic Inorganic Chemistry*, Wiley, 3rd ed., 1995; G.W. Parshell and S.D. Ittel, *Homogeneous Catalysis*, Wiley Interscience, 2nd edn., 1992; B.R. James, *Inorg. Chim. Acta, Rev.*, (1970) 73.
[2] T.V. Ashworth, A.A. Chalmers, E. Meintjies, H. Oosthuizen and E. Singleton, *J. Organomet. Chem.*, *286* (1985) 237; *Organometallics*, *3* (1984) 1485; T.V. Ashworth, A.A. Chalmers, D.C. Liles, E. Meintjies, H. Oosthuizen and E. Singleton, *J. Organomet. Chem.*, *284* (1985) C19.
[3] For example, G. Costa, in G. Allen and J.C. Bevington (eds.), *Comprehensive Polymer Science*, Vol. 4, Pergamon Press, Oxford, 1989, pp. 155–161.
[4] Y. Kishimoto, P. Eckerle, T. Miyatake, T. Ikariya and R. Noyori, *J. Am. Chem. Soc.*, *116* (1994) 12131.
[5] (a) C. Bianchini, M. Peruzzini, F. Zanobini, P. Frediani and A. Albinati, *J. Am. Chem. Soc.*, *113* (1991) 5453; (b) P. Barbaro, C. Bianchini, M. Peruzzini, A. Polo and F. Zanobini, *Inorg. Chim. Acta*, *220* (1994) 5; (c) C. Bianchini, P. Frediani, D. Masi, M. Peruzzini and F. Zanobini, *Organometallics*, *13* (1994) 4616.
[6] Y. Wakatsuki, N. Koga, H. Yamazaki and K. Morokuma, *J. Am. Chem. Soc.*, *116* (1994) 8105.
[7] J. Wolf, H. Werner, O. Serhadli and M.L. Ziegler, *Angew. Chem., Int. Ed. Engl.*, *22* (1983) 414; A. Höhn, H. Otto, M. Dziallas and H. Werner, *J. Chem. Soc., Chem. Commun.*, (1987) 852.
[8] (a) M.O. Albers, D.J.A. De Waal, D.C. Liles, D.J. Robinson and E. Singleton, *J. Organomet. Chem.*, *326* (1987) C29; (b) M.O. Albers, D.J.A. De Waal, D.C. Liles, D.J. Robinson, E. Singleton and M.B. Wiege, *J. Chem. Soc., Chem. Commun.*, *22* (1986) 1680.
[9] Presented, in part, at the *National Physical Symposium of the South African Chemical Institute, Dikhololo, Transvaal, July, 1988.*
[10] G. Albertin, P. Amendola, S. Antoniutti, S. Ianelli, G. Pelizzi and E. Bordignon, *Organometallics*, *10* (1991) 2876 and references cited therein.
[11] P.R. Hoffman and K.G. Caulton, *J. Am. Chem. Soc.*, *97* (1975) 4221.
[12] R.G. Pearson, *J. Am. Chem. Soc.*, *91* (1969) 4947; M. Elian and R. Hoffmann, *Inorg. Chem.*, *14* (1975) 1058.
[13] T.V. Ashworth, A.A. Chalmers and E. Singleton, *Inorg. Chem.*, *24* (1985) 2125.
[14] G. Jia, A.L. Rheingold and D.W. Meek, *Organometallics*, *8* (1989) 1378; G. Jia, J.C. Gallucci, A.L. Rheingold, B.S. Haggerty and D.W. Meek, *Organometallics*, *10* (1991) 3459.
[15] A.G. Orpen, L. Brammer, F.H. Allen, O. Kennard, D.G. Watson and R. Taylor, *J. Chem. Soc., Dalton Trans.*, (1989) S1.
[16] T.V. Ashworth, M.J. Nolte, E. Singleton and M. Laing, *J. Chem. Soc., Dalton Trans.*, (1977) 1816.
[17] S.J. La Placa and J.A. Ibers, *Inorg. Chem.*, *4* (1965) 778.
[18] A.J. Blake, N.R. Champness, R.J. Forder, C.S. Frampton, C.A. Frost, G. Reid and R.H. Simpson, *J. Chem. Soc., Dalton Trans.*, (1994) 3377.
[19] S.D. Ittel and J.A. Ibers, *Adv. Organomet. Chem.*, *14* (1976) 33.
[20] A.C.T. North, D.C. Philips and F.S. Matthews, *Acta Crystallogr., Sect. A*, *24* (1968) 351.
[21] G.M. Sheldrick, *Computing in Crystallography*, Delft University Press, 1978, pp. 32–42.